Accepted Manuscript

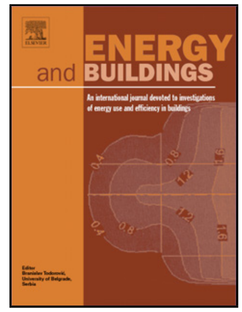

Title: Multi Objective Receding Horizon Optimization for Optimal Scheduling of Hybrid Renewable Energy System

Authors: Atefeh Behzadi Forough, Ramin Roshandel

PII: S0378-7788(16)31740-6
DOI: http://dx.doi.org/doi:10.1016/j.enbuild.2017.06.031
Reference: ENB 7694

To appear in: *ENB*

Received date: 1-12-2016
Revised date: 25-5-2017
Accepted date: 12-6-2017

Multi Objective Receding Horizon Optimization for Optimal Scheduling of Hybrid Renewable Energy System

Atefeh Behzadi Forough, Ramin Roshandel[1]

Department of Energy Engineering, Sharif University of Technology, P.O. Box 11365-9567, Tehran-Iran.

Tel.: +98 (21) 6616 6127; Fax: +98 (21) 6616 6102

Email: roshandel@sharif.edu

[1]Corresponding author

Research Highlights

- The concept of multi objective receding horizon optimization (MO-RHO) is presented
- The measured data profiles are implemented into energy management system
- The optimal operation scheduling of hybrid renewable energy system is presented
- The effect of length of prediction horizon on optimal scheduling is analyzed
- The effect of seasonal variations on economic performance is investigated

Abstract

In this paper, a methodology for energy management system (EMS) based on the multi-objective receding horizon optimization (MO-RHO) is presented to find the optimal scheduling of hybrid renewable energy system (HRES). The proposed HRES which is experimentally installed in educational building comprising the PV panels, wind turbine, battery bank and diesel generator as the backup system. The data acquisition system provides input profiles for receding horizon optimizer. A mixed-integer convex programing technique is used to achieve the optimal operation regarding to two conflicting operation objectives including diesel fuel cost and battery wear cost. The Pareto frontiers are presented to show the trade-offs between two operation objective functions. Analysis of obtained results demonstrates that the system economic and technical performance are improved using longer prediction horizon. The results show that using longer time view (from 6 hr to 24 hr) the total share of renewable energy in supplying weekly demand can be improved up to 18.7%. Therefore, the proposed methodology can manage system to make a better use of resources resulting in a better system scheduling. The sensitivity analysis also demonstrates the effectiveness of seasonal variations of available renewable resources on the optimal operation scheduling.

Keywords: Multi objective receding horizon optimization, Energy management system, Optimal scheduling, Hybrid renewable energy system

Nomenclature

P	Power flow, (W)	$F_i(x)$	Objective function
A	area, (m^2)	F_i^{trans}	non-dimension objective function
G	solar irradiation (W/m^2)	CL_i^+	relative closeness of Pareto solutions
T	Temperature (°C)	d_i^+	Pareto distances to the positive solution
C_P	coefficient of wind turbine performance	d_i^-	Pareto distances to the negative solution
V	wind speed (m/s)	C_{Ope}	operation cost ($)
$P_{W,r}$	wind turbine rated power (W)	C_f	diesel fuel cost ($/liter)
V_C	cut-in wind speed (m/s)	N	Horizon number
V_r	Rated wind speed (m/s)	M	relaxation constant parameter
V_f	cut-off wind speed (m/s)	δ	integer variable
E	Energy (Wh)	**Subscripts**	
t	Time (hr)	PV	Photovoltaic
SOC	State of charge	c	Cell
$E_{Bat,max}$	Battery capacity (Wh)	W	Wind turbine
DOD	Depth of discharge	Bat	Battery
λ_L	estimated throughput (cycles Wh)	ch	Charge status
CTF	cycles to failure	dis	discharge status
$C_{Bat,w}$	Battery wear cost ($/Wh/cycle)	Con	conversion system
$C_{Bat,life}$	net present values of battery ($)	Sto	storage system

C_{Bat}	cost of battery ($)	n	number of conversion system
r	discount rate	m	number of storage system
n	System lifetime (year)	**Greek symbols**	
$Fuel_{DG}$	diesel fuel consumption (Liter)	η	efficiency
P_{r-DG}	diesel generator rated capacity (W)	η_{PV}	PV module efficiency
α_{DG}	diesel fuel consumption coefficients (l/kWh)	$\eta_{T,PV}$	PV thermal efficiency
β_{DG}	diesel fuel consumption coefficients (l/kWh)	α	PV temperature coefficient
y	System capacity (W, Wh)	ρ	air density (kg/m^3)
x	State variable	min	minimum
u	Control variable	max	maximum
U	Utility function	DG	diesel generator
w	weighted factor		

1. Introduction

Climate change, depletion of fossil fuels and increase of electricity demand necessitate the use of local energy potentials which cause renewable energy system (RES) to be an efficient and feasible solution [1]. Hybrid renewable energy system (HRES) is an integrated system which simultaneously uses different energy resources including renewables or non-renewables. HRES is consisted of several sub-systems which can be expressed as generation, storage and backup systems. The application of HRES has various advantages such as decrease the fluctuations in the generation side, operation cost and environmental emissions. It also increases the system reliability. In HRES, the required electricity demand at each time step should be satisfied by various energy flows from different renewable energy generation, storage or backup systems. The determination of these energy flows during the operation time affects the economic performance and reliability of HRES. This justifies the application of energy management system (EMS) to meet the demand profiles while optimizing the technical and economic performance related to operation scheduling of HRES. Therefore, the schedule of HRES should be optimized using operation optimization procedure to better manage the energy flows. The first principle of EMS is to determine power flows corresponding to renewable and non-renewable generation resources while the second principle is based on the controlling and management of HRES operation variables (such as state of charge in storage systems) [2].

Recently, the numbers of researches which are focused on scheduling optimization of HRES are growing. There are two main approaches in the literatures for operation optimization to determine the scheduling strategy in HRES: 1) conventional optimization and 2) receding horizon optimization (RHO).

In the first approach, the historical data for the entire operation life time including the availability of renewable resources as well as demand load profiles are provided. All the input data are imported and the optimizer tries to find the optimal operation for the whole operation lifetime. In this case, the optimization procedure is performed only one time and the variability of input profiles (weather/demand) during operation time cannot be considered in the optimization procedure.

Numerous previous literatures have attempted to achieve the optimal operation scheduling of energy system through EMS. The proposed techniques which are applied for operation optimization in conventional approach include mathematical programming (mixed integer linear programing) [3,4], heuristic methods (genetic algorithm, particle swarm optimization, fuzzy algorithm, artificial neural network) [5-9], aging-based modeling [10,11], agent-based modelling [12-14], stochastic approach [15] and priority rules [16].

Garcia et al. [2,18,19] considered a HRES which is composed of PV/Wind as primary energy sources and hydrogen subsystem and battery as the energy storage systems. They present a long-term operation optimization framework for HRES based on three EMSs. The objective functions regarding each EMS are minimization of energy storage utilization cost, maximization the energy storage system efficiency and maximization the lifetime of the energy storage devices. The main goal of long term optimization is to achieve the efficient use of renewable energy resources and scheduling the energy storage systems to store and release the power flows in different time steps. Optimal energy management system for an off grid PV/DG/battery and PV/Wind/DG/battery hybrid power systems has been presented by Tazvinga et al. [20-22]. The optimization procedure minimizes the battery wear and fuel costs to determine the optimal power flow regarding availability of renewable energy resources, battery state of charge and load demand. The optimal solutions for equally weighted objectives and for a case with larger weight to battery wear cost are compared and analyzed. Pascual et al. [23] proposed the energy management methodology for a residential grid-connected microgrid which is consisted of PV, wind turbine and battery energy storage. The proposed control strategy allows the control of power exchange through a battery and utility grid using the charge level in battery, power flows in each node, load and available renewable generation forecasts as input data. The system simulation shows that the EMS results have an improvement in grid power profile regarding the given storage system. Also, they experimentally validated their proposed energy management strategy by the Renewable Energy Laboratory at the UPNa. An operation optimization methodology for maximization the economic objective regarding the market prices and predicted renewable resources is proposed by Chen et al. [24]. The systematic control strategy of renewable energy system to make maximization the economic objective is implemented through the operation optimizer in their methodology. The capability of computational methodology has been illustrated regarding the optimization results for two configurations of HRES. The comparison between economic performance of proposed flexible operation strategy and constant operation strategy shows the advantage of their proposed optimizer. Finally, the sensitivity analysis regarding two parameters (prediction error and variability of market prices) is presented. Marzband et al. [25] and Ikeda et al. [26] presented the new operation optimization strategy to schedule of a HRES. In [25] the capability and effectiveness of real time operation optimization applications are validated using experimental setup. The uncertainty of renewable energy resources as well as demand changes are considered in [26].

Multi objective optimization can be used to show the trade-offs between conflicting objectives. Different objective functions can be optimized regarding operation strategy to achieve the optimal scheduling with respect to operator preferences. There are several researches which performed the multi objective operation optimization in their proposed EMS [27-28]. Recently, the technique for order preference by similarity to an ideal solution (TOPSIS) method has been applied as a tool to determine an optimal solution which is closet to positive ideal solution and farthest to the negative ideal solution among the Pareto solutions in a multi objective optimization. TOPSIS technique has been used in various studies which are related to decision making to calculate the optimal solution [29-30]. Li et al. [31] presented an operation optimization framework for a building cluster which optimizes the scheduling through particle swarm algorithm based multi-objective optimization. The Pareto frontiers have been achieved through multi objective optimization for making trade-off between thermal comfort level and energy cost saving as two objective functions. A multi-objective operation optimization is proposed by Di Somma et al. [32] to obtain the optimal scheduling of the HRES. Energy costs and environmental impacts are considered as two objective functions. Best possible trade-offs between objective functions are presented using weighted sum of operation cost and environmental emissions.

In the second approach (RHO), the real time profiles for specific horizon are provided at each time step to optimize the operation scheduling. Receding horizon optimization approach is applied to EMS and the real-time operation optimization of HRES is achieved. In receding horizon methodology, decision variables (control variables) are optimized in the moving time horizon as the optimal trajectories. These trajectories are updated on an hourly/daily timescale and then the results are returned as state variables for further real-time optimization in the next time step. RHO methodology has been applied to the determination of optimal operation scheduling for the process industries [33-34]. One of the main advantages of RHO in comparison with conventional optimization approaches is the ability of considering the uncertainties and intermittent behavior of renewable energy resources in operation optimization of HRES. Therefore, the implementation of RHO on HRES can improve the technical and economic justification of such systems.

Feroldi et al. [35] proposed an energy management system to optimize the scheduling of a solar/wind hybrid renewable energy system which uses batteries and fuel cells as the storage system. Receding horizon optimization is applied with prediction of future renewable generation regarding load profiles and the battery state of charge. The application of RHO decreases loss of power supply probability up to 88% in comparison to the case of without prediction. Prodan et al. [36] presented a reliable energy management framework for a microgrid using RHO methodology. An on-grid microgrid includes a wind turbine and a battery bank as the storage system. The main objective of this work is to optimize the operation scheduling of battery system to minimize the operation cost. It is concluded that the proposed framework is an effective approach to optimize the scheduling and management of HRES using resource/demand profiles, objective function and constraints. Petrollese et al. [37] proposed a novel energy management strategy for a renewable hydrogen energy system. The energy management strategy is developed to achieve the long term optimal planning as well as short-term optimal energy scheduling. Several experimental studies show that the application of energy management system can enhance the reliability and technical performance of the HRES while can reduce the system operation cost. Wang et al [38] presented the receding horizon optimization methodology for energy management of HRES in the chlor-alkali chemical unit. The energy management framework is proposed in order to supply the demand with the objectives of minimizing the operation cost and environmental emissions. The on-grid HRES includes PV, wind turbine and fuel cell to supply demand load. Sensitivity analysis are conducted to illustrate the effect of key parameters on the operation of HRES. Demand side energy management is also added to their proposed EMS to capture the effect of demand profile changes on the optimal scheduling in [39]. In the other work, a real time optimization methodology is developed to achieve optimal scheduling electricity supply system [40]. An EMS is also proposed for realization the economic and environmental objectives while meeting production requirements. Demand response strategies are implemented into their methodology to improve the system reliability. A receding horizon optimization framework based on two stage methodology for building energy management (BMS) is developed by Gruber et al. [41]. The proposed HRES includes PV, diesel generator (DG) and battery storage system which is applied to meet the dispachable/non-dispachable demand loads. The optimal scheduling management for a medium-size hotel which is simulated in an experimental setup is developed through the proposed framework. The results illustrate that the proposed EMS can be implemented in the flexible power scenarios and various desirable conditions.

In this paper, the novel energy management system (EMS) based on receding horizon optimization is presented. Multi objective receding horizon optimization (MO-RHO) is proposed to show the trade-offs between conflicting operation objective functions. Battery wear cost and diesel fuel cost are two objective functions which are implemented in a HRES which includes PV, wind turbine, batteries and a diesel generator as the backup system. The required data profiles (weather and demand) for MO-RHO are imported from a real experimental setup which is installed at department of energy engineering building, Sharif University of Technology (SUT) to meet the required demand load. The imported data profiles are used in a mixed integer convex optimization (MICO) framework which is solved using CVX solver to achieve the optimal operation strategy. The sensitivity analysis is also performed to analyze the effect of prediction horizon and seasonal variations of renewable generation profiles on the optimal operation scheduling.

In short, the main contributions of proposed paper are as follows:

- The concept of multi objective receding horizon optimization (MO-RHO) for optimal scheduling of buildings is presented.

- The measured data profiles are implemented into real time optimization framework at each moving prediction horizon.
- The share of direct/indirect renewable energy resources in supplying the demand load of proposed building is analyzed to capture the effect of length of prediction horizon of RHO methodology and seasonal variations of generation profiles on optimal scheduling.

2. Problem under study

The configuration of hybrid renewable energy system which is considered in this work is illustrated in Fig. (1). The EMS framework is implemented into HRES as a case study for assessing the proposed EMS. The HRES includes PV and wind turbine as primary renewable resources, diesel generator for backup system as well as battery bank for storing the surplus energy and improving the HRES reliability. All HRES sub-systems and loads are connected together through a DC bus by means of specified converters as a stand-alone system. The battery storage system and DG compensate the lack of renewable generation power for supplying the demand load in HRES. The y_i denotes the size of specific sub-system and P_i (t) denotes the various power flows in each time step which are specified by the energy management system. The main goal of the proposed EMS is determination of power flows as the control variables (P_{Bat} and P_{DG}) while the demand load is completely satisfied and operation cost is minimized. In this study, the weather and demand profiles which are imported in proposed EMS as the input parameters are measured by HRES experimental setup. The weather data including solar radiation, wind speed, PV and ambient temperatures are measured by sensors in HRES experimental setup which is installed in educational building at Tehran-Iran (latitude: 35.41, longitude: 51.19).

A hybrid renewable energy system is experimentally installed at the roof of department of energy engineering building to show the viability of our methodology using measured profiles as the input data for the proposed EMS. As the Fig. (2) shows, the installed HRES includes two renewable power generation sub-systems: the rooftop photovoltaic system and a three bladed horizontal axis wind turbine. The HRES also includes charge controllers, battery bank and a power island. In summary, the detail of the commercially renewable energy generators, the battery bank and the other devices comprising the installed HRES, are presented in Table (1). The lead acid battery is designed by 6 cells of 1.8 V. The battery management system (BMS) which is connected to power island by RS485 interface is implemented to monitor the state of charge (SOC) and the state of health (SOH) of battery bank and keep the battery from risky operation using battery temperatures and voltages. The installed HRES provides the possibility of implementation and verification of energy management system to increase the system productivity and capability. The measured profiles including solar irradiation, wind speed and PV cell/ambient temperatures with the accuracy of ±10W/m^2, ±1m/s, ±1°C and ±1°C respectively, are transmitted using RS485 protocol to a communication interface (sample rate: 10s). The developed data logging and monitoring system lets us to monitor the real-time energy flows from resources to final uses. It is expected that the department desired electricity loads are practically supplied by the installed HRES setup.

3. Problem formulation

The first step to develop the energy management system of HRES is the analysis of different sub-system performances based on the input data profiles. For this goal, the input/output technical model which calculates the power generation at each time interval according to experimental design parameters and measured input data are required. The technical model of HRES is consisted of four main sub-models. These sub-models are PV, wind turbine, battery and diesel generator which are implemented through the hourly time interval analysis of weather data profiles (solar irradiation, wind speed and PV/ambient temperatures) from experimental setup. At the same step, the operation cost model which includes the battery wear and diesel fuel costs are presented as two operation objective functions.

3.1. Renewable energy generation systems

Solar and wind are considered as two renewable energy resources which are converted to electricity by PV module and wind turbine.

The power produced by a photovoltaic module can be calculated using Eqs. (1) and (2) [42]:

$$P_{PV}(t) = \eta_{PV}\eta_{T,PV}A_{PV}G(t) \tag{1}$$

$$\eta_{T,PV}(T_c) = \eta_{T,PV}(25^{0}C)[1+\alpha(\eta_T)(T_c-25^{0}C)] \tag{2}$$

Where, P_{pv} is the output power, G(t) is hourly total solar irradiation, η_{PV} is PV efficiency and A_{PV} is the panel area (m^2). PV cell temperature which is measured using temperature sensor is used to calculate PV module efficiency. The G(t) and T_C which are experimentally measured are used as input profiles in receding horizon operation optimization. The other PV model parameters are given in Table (2) based on installed experimental setup.

The wind turbine converts wind kinetic energy to electrical energy. The generated power from a wind turbine is determined by Eq. (3) [43].

$$P_W(t) = \begin{cases} 0 & V < V_C \\ \frac{1}{2} C_P \rho A_W V^3(t) & V_C < V < V_r \\ P_{W,r} & V_r < V < V_f \\ 0 & V > V_f \end{cases} \tag{3}$$

C_p is the coefficient of performance of wind turbine. A_W is the rotor swept area, ρ is air density, $P_{W,r}$ is the wind turbine rated power, V_C, V_r and V_f are cut-in, rated and cut-off wind speeds, respectively. The main characteristics of the installed wind turbine are depicted in Table. (2). V(t) is hourly wind speed which is experimentally measured in time step (t).

3.2. Energy storage system

The energy storage system is consisted of lead-acid battery banks which are charge or discharge regarding the renewable generation power (PV/wind) and the load profile at each time step. The following dynamic equation is used to describe the energy stored in battery as the state variable.

$$E_{Bat}(t+1) = \begin{cases} (1-\tau)E_{Bat}(t) + P_{ch}(t)\eta_{ch} \\ (1-\tau)E_{Bat}(t) - \frac{P_{dis}(t)}{\eta_{dis}} \end{cases} \tag{4}$$

Where, E_{Bat} (t+1) and E_{Bat} (t) are the amount of energy stored in battery at time step t+1 and t, η_{bat} and η_{dis} are the battery efficiencies including charge/discharge efficiencies. τ is self-discharge coefficient and $P_{ch}(t)$/ $P_{dis}(t)$ are charged/discharged power flows in each time step (t). SOC_{min} and SOC_{max} are lower and upper limits of battery state of charge (SOC) and DoD is the depth of battery discharge [44].

$$SOC_{min} \times E_{Bat,max} \leq E_{Bat}(t) \leq SOC_{max} \times E_{Bat,max} \tag{5}$$

$$SOC_{min} = (1 - DOD) \tag{6}$$

The power flows from/to batteries are restricted by Eqs. (7) and (8) [44].

$$0 \leq P_{ch}(t+1) \leq (SOC_{max} \times E_{Bat,max}) - E_{Bat}(t) \tag{7}$$

$$0 \leq P_{dis}(t+1) \leq E_{Bat}(t) - (SOC_{min} \times E_{Bat,max}) \tag{8}$$

The operation cost of the batteries is one of the significant HRES operation costs that has not been comprehensively investigated in the conventional EMS studies. The lead acid batteries have been used in the installed HRES. Post-processing and performance degradation models are two common lifetime models for lead acid batteries. The post-processing model (PPM) doesn't include a performance model while the performance degradation model (PDM) integrates a performance model with lifetime considerations and so that the battery performance can be investigated based on the utilization scheduling of the battery [45]. Ah-throughput and cycle counting are two lifetime consumption methods in PDM which are required to calculate the battery operation cost.

In this study, the Ah-throughput counting method is employed to determine the battery lifetime consumption [45]. The mentioned method assumes that the fixed quantity of energy can be cycled in a battery storage system before the battery needs replacement. In this method, λ_L is the estimated throughput over a battery storage system lifetime and almost specified by the DoD-cycles to failure (CTF) curve (which is provided by the manufacture) and the maximum capacity of battery ($E_{Bat,max}$). λ_L is presented as Eq. (9) [20]:

$$\lambda_L = \mathrm{DOD} \times \mathrm{CTF} \times \mathrm{E_{Bat,max}} \tag{9}$$

The battery capacity degradation depends mainly on charging/discharging scheduling and battery DoD [20]. To obtain the operation cost of battery bank, the battery utilization cost per cycle ($/kWh/cycle) is needed. The battery wear cost ($C_{Bat,w}$) is calculated by dividing the battery lifetime cost which is defined by sum of the replacement cost of battery bank during the HRES lifetime ($C_{Bat,life}$) (Eq. (13)) to the net energy consumption of battery bank (λ_L) as shown in Eq. (10) [27]. $C_{Bat,life}$ is the net present values (NPV) [46] of battery replacement cost that occurred in each replacement time of battery in the duration of HRES operation (20 year) [44].

$$C_{Bat,w} = \frac{C_{Bat,life}}{\lambda_L} \tag{10}$$

$$C_{Bat,life} = \sum_{n=5,10,15} C_{Bat} \times \frac{(r+1)^n - 1}{r \times (r+1)^n} \tag{11}$$

3.3. Backup system

Diesel generators (DG) are considered as the backup system in the proposed hybrid renewable energy systems. DG converts the chemical energy stored in diesel fuel into electricity which is used to supply the required load. DG power in addition to battery charge/discharge flows are the independent variables which can be directly controlled in HRES. DG fuel consumption is the major portion of operation cost in the HRES which is a function of generator size and the load at each time step. Thereupon, the fuel consumption of a DG can be calculated using Eq. (12) [43].

$$Fuel_{DG}(t) = \alpha_{DG} P_{r-DG} + \beta_{DG} P_{DG}(t) \tag{12}$$

$P_{r\text{-}DG}$ is the rated capacity in installed setup while P_{DG} is the practical output power of DG in time step (t). Also, α_{DG} and β_{DG} are diesel fuel consumption coefficients. Fuel price is averagely considered to be 1.2 $/L [44]. The technical and economical parameters used in battery and DG models are given in Table (3).

4. MULTI OBJECTIVE RECEDING HORIZON OPTIMIZATION

In this study, the concept of multi objective receding horizon optimization (MO-RHO) is proposed which implements the multi objective approach into receding horizon optimization.

The mathematical framework of energy management methodology is presented in Fig. (3). The EMS framework is consisted of three sections: 1) performance model, 2) operation cost model and 3) receding horizon optimization. The input parameters of EMS include technical and economic parameters as well as available energy sources and demand profiles which are imported from experimental setup at each prediction horizon. The y is the capacity vector of the different devices in HRES including PV, Wind and battery bank. In this paper, the practical values of the installed HRES capacities (are presented as y in the framework input) are used for the operation optimization. At the first section, using input profiles the output energy flows are determined for conversion and storage systems (P_{Con}, P_{Sto}). In this section, the simulation models are used for determination of generation power profiles in order to keep and generalize the flexibility of our proposed framework. At the second section, the corresponding operation cost of HRES sub-systems regarding the output energy flows is determined. The operation cost is consisted of the fuel cost and battery wear cost which are two main operation objective functions in receding horizon optimization. At the third section, the operation optimization is performed using receding horizon optimization technique to achieve optimal scheduling. The receding horizon optimizer is applied at each time step during the operation time of HRES. At each time step, the measured demand and weather profiles for the specific horizon regarding the number of future time steps are imported to the optimization solver. The mixed integer convex programing is used to optimize the control variables. It is proven that the convex optimization guarantees the achieved optimal solution is unique and global. Therefore, the resulted optimal schedule of system is globally optimal and consequently the objective function (diesel fuel cost and battery wear cost) which are related to this scheduling will be the global optimal solution. The amount of energy in battery (E_{Bat}) is the state variable which is calculated at each time step and used as initial variable for future time step. The optimizer tries to optimize the operation cost as the objective function regarding related constraints. Dynamic constraints provide time relationship between state variables while the technical constraints determine the feasible region of the optimization problem. The obtained trajectories in each horizon include battery charge/discharge power flows (P_{ch}/P_{dis}) and DG generation power (P_{DG}) which are the control variables and amount of energy in battery as the state variable (E_{Bat}). The first values of the power trajectory vectors are implemented as the optimal solution for time step (t). In the next time step, the input profiles as well as trajectories are updated and new initial conditions and profiles are implemented into the next moving horizon till the final time step number is reached.

Finally, the main output of the receding horizon optimization is to determine the optimal operation scheduling using the available renewable resources based on the desirable objective functions. Fuel cost is the conventional operation objective which affects the economic performance of the HRES. However, the battery wear cost which can be optimally tuned imposes the significant cost on operation cost of HRES. Therefore, to achieve the optimal scheduling these two objective functions should be simultaneously considered in the optimization procedure. These objectives are conflicting since the first objective determines the non-renewable resource utilization while the second objective relies on the indirect renewable energy utilization.

In this context, multi objective optimization technique can be implemented into receding horizon optimization problem to show the trade-offs between optimal solutions regarding two operation objective functions. In this study, the weighted global criterion method which is one of the conventional methods for multi objective optimization problem is used. In this method, all desired objectives are combined for making one single objective [46]. The weighted factors are assigned to the different objectives to show the model preferences. The general utility function (U) is weighted exponential sum as is presented in Eq. (13) [47].

$$U = \sum_{i=1}^{f} w_i \times [F_i(x)]^p, \quad F_i(x) > 0 \ \forall i \tag{13}$$

Where w_i is the weighted factor which follows as Eq. (14) and f is the number of objective functions. Usually one is considered as a fixed amount for p then, the operator tunes w to illustrate the preferences a priority or w systematically is modified for obtaining the Pareto frontiers. As the dimensions of considered objectives are different, usually it is useful to transform the original objectives. One of the most common approaches for solving this problem is presented in Eq. (15) [17].

$$\sum_{i=1}^{f} w_i = 1 \tag{14}$$

$$F_i^{trans} = \frac{F_i(x)}{|F_i^{max}|} \tag{15}$$

After identification of Pareto optimal points, the TOPSIS method is applied for ranking these solutions regarding the shortest distance from ideal positive solution and farthest distance from negative ideal solution. For this aim, the distances of the each Pareto solution to the positive and negative ideal solutions (d_i^+ and d_i^-), are calculated [30]. Afterward, the relative closeness of Pareto solutions (CL_i^+) to the ideal solution are calculated from Eq. (16) and ranked based on the relative descending order of Pareto solutions [30].

$$CL_i^+ = \frac{d_i^-}{(d_i^+ + d_i^-)} \qquad 0 \le CL_i^+ \le 1 \qquad i = 1,2,\dots,m \tag{16}$$

Where m is the number of Pareto solutions. Each solution which has the largest value of CL_i^+ is considered as the optimal solution based on the TOPSIS method.

To determine the optimal scheduling of HRES in the MO-RHO methodology, the different desired objectives with the related dynamic and state constraints are applied using the mathematical modeling of an optimization procedure. The receding horizon method optimizes the control variables in each time step regarding deterministic multi objective optimization. Optimal trajectories are obtained as the output in related time step and the first values of these trajectories are reported as final optimal solution in current time step. Then the obtained trajectories are used as the initial condition for next time step. Finally, the operator can alter the weighted factor for showing the preferences to determine the Pareto solutions.

In this study, the considered operation objectives of HRES are battery wear cost and diesel fuel cost which are optimized in the specific horizon through the multi objective optimization technique. To solve the MO-RHO problem and manage the operation of HRES, the dynamic formulation is considered. The **u**=[P_{DG} , P_{ch} , P_{dis}] and **x**=[E_{Bat}] are the control variable and the state variable (feedback variable) vectors which are imposed in the receding horizon optimization model. The model of proposed optimization for each time step (t) is formulated as Equations (17) and (18).

$$min \ \ \sum_{i=t}^{t+N-1} C_{Ope}\left(u(i|t)\ ,x(i|t)\right) \tag{17}$$

$$\begin{aligned}
&C_{Ope}\big(u(i|t),x(i|t)\big) = w \times (C_f\ Fuel_{DG}(i|t)) + (1-w) \times (C_{Bat,W}\ [P_{ch}(i|t) + P_{dis}(i|t)])\\
&subject\ to \quad \forall\, i \in [t\ ,t+N-1]\\
&P_{Con,n}(i|t) + P_{Sto,m}(i|t) \geq D(i|t) \qquad n = PV, wind, DG\ \ \&\ \ m = battery\\
&E_{Bat}(i+1|t) = (1-\tau)E_{Bat}(i|t) + P_{ch}(i|t)\eta_{ch} - \frac{P_{dis}(i|t)}{\eta_{dis}}\\
&SOC_{min} \times {y^*}_{Bat} \leq E_{Bat}(i|t) \leq SOC_{max} \times {y^*}_{Bat}\\
&0 \leq P_{ch}(i+1|t) \leq (SOC_{max} \times {y^*}_{Bat}) - E_{Bat}(i|t)\\
&0 \leq P_{dis}(i+1|t) \leq E_{Bat}(i|t) - (SOC_{min} \times {y^*}_{Bat})\\
&P_{ch}(i|t) \leq M \times \delta(i|t)\\
&P_{dis}(i|t) \leq M \times (1-\delta(i|t))
\end{aligned} \tag{18}$$

$$0 \leq P_{Con,n}(i|t) \leq {y^*}_n \qquad n = PV, wind, DG$$

Where α (i|t) generally indicates the value of α parameter at the time step i, $\forall\ i \in [t\ , t + N - 1]$. α (t|t) denotes the optimal parameter at the current time step (t) while α (i|t), $\forall\ i \in [t + 1\ , t + N - 1]$ is the predicted parameter using the information available at time step (t), over the future time steps that may or may not be implemented in the next time steps. N represents the length of the receding prediction horizon, i is the counter of time step in the specific horizon which is updated in each horizon and y^* is the actual sizing of the HRES components which are determined using installed experimental setup. Also, δ denotes the binary variable (δ∈ $\{0,1\}$) and M is a relaxation constant parameter which is significantly more than the other parameters.

The related constraints generally include supplying the hourly demand, dynamic equation over the amount of energy in battery as the state variable, the maximum and minimum limitations of energy stored in battery bank and the power rate limit on charge/discharge of battery bank. Also, the mixed integer constraints are implemented to the optimization model to consider the physical limitation of the charge/discharge state of battery bank. The produced power from renewable energy generators are limited by the actual sizing which are determined from the experimental setup.

5. Result and discussion

In this section, the results of MO-RHO methodology are presented. To show the capability of the proposed framework, the real practical profiles are measured and collected in developed database. The measured profiles from experimental setup for a sample week (first week of January) are implemented into the proposed energy management system. The input data which are presented in Fig. (4) include solar irradiation, wind speed, PV cell and ambient temperatures.

The receding horizon optimizer tries to find the optimal trajectories and solutions in each moving horizon regarding measured data profiles. Fig. (5) illustrates the hourly optimal power flows and related trajectories in moving horizons for sample day (hours: 24-48).

In Fig. (5-A), (5-B) and (5-C) the optimal power flows for three control variables including diesel generator and battery charge/discharge are presented. The energy analysis in the considered sample day shows that DG optimally supplies the demand load at midnight's hours (hours 26-31) when the power from PV and wind turbine are not sufficient. Batteries are charged during the midday hours (hours 36-39) when the solar power is more than the demand load. Battery discharge is happened from sunset to the midnight hours (hours: 40-44) since there are not renewable resources to supply demand while the batteries are sufficiently charged.

Fig. (5-A) shows DG optimal power generation in each time step with two sample trajectories for time steps 26 and 27. As it can be seen, in time step 26, the optimal trajectory for six future hours is presented which its trend is generally followed by the trajectory corresponding to the time step 27. The first values in each trajectories corresponding to each time steps are implemented as the optimal DG power flows which make the final receding horizon optimization solution in operation time. Also, the calculated state variables (amount of energy in batteries) in each time step are applied as the initial values for receding horizon optimization in the next time step. It is worthy to indicate that using receding horizons it is possible to capture the variation of load in future time steps (Hour: 31) and generation profiles to estimate the optimal power flows.

Fig. (5-B) and (5-C) show the optimal battery charge/discharge optimal power flows with two sample trajectories (time steps: 36 and 37 for charge and time steps: 41 and 42 for discharge). The optimal initial values at each trajectory are reported as the optimal solution and the optimal trajectories of control and state variables in each time step are implemented as the initial condition for future receding optimization.

Fig. (6) shows the measured daily demand profile which should be supplied by proposed HRES. This includes the library lighting, personal computer, roof day/night lighting, and communication interface devises. There are three ways to supply the demanded load which called direct renewable, indirect renewable (discharge from batteries) and diesel generator. As indicated in this figure, by increasing the length of prediction horizon, the total share of renewable energy (direct renewable + indirect renewable) in supplying the load is increased. This is mainly due to the longer vision of receding horizon optimizer which leads to better schedule of charge/discharge of batteries. When the longer length of horizon is considered, more view of future can be captured and therefore it will be possible to achieve the optimal schedule in current time step based on satisfying the total constraints over the longer length of proposed horizon.

Fig (7) presents the weekly demand profile which is supplied by HRES. As it can be seen, by increasing the length of horizon from 6 to 12 hours, diesel generator power flow is decreased from 41.1 kWh to 24.3 kWh entire the week. It means that using longer prediction horizon (from 6 to 12 hours) the diesel consumption and related environmental impact are decreased up to 12.82%.

The operation cost of HRES is divided into two main parts including diesel fuel cost and the battery wear cost. Increasing the share of renewables in supplying the demand, leads to decrease of diesel fuel consumption. Therefore, there is a trade-off between these two objective functions. As indicated before increasing the length of prediction horizon leads to better managing of battery scheduling and increases the share of renewable energy. However, this could increase the battery cycling and consequently the battery utilization cost is increased. Fig (8), shows the effect of length of prediction horizon on conflicting behavior of diesel fuel cost and the battery wear cost. Recent researches have proven that is a trade-off between selection of length of prediction horizon and CPU running time [39]. As the length of horizon increases the corresponding optimal operation cost decreases while simultaneously the time for running the optimization problem increases. As the RHO is the online optimization procedure and must be run in each time step, the running time is an important issue. Therefore, there is a trade-off between these two factors and decision maker must decide based on need and existence conditions.

The multi objective optimization technique which is applied to receding horizon optimization (MO-RHO) is a powerful decision making tool to achieve the optimum operation of HRES based on multiple objective functions. The trade-offs between two conflicting objectives (diesel fuel cost and the battery wear cost) regarding different weighted factors are presented as the Pareto frontiers. Fig. (9) shows the Pareto frontiers which are obtained using different weighted factors for two objective functions. As it can be seen, by increasing the weighted factor which means that diesel fuel cost is more important than the battery wear cost, the share of renewable energy is increased. Therefore, to study the effect of battery wear cost on operation schedule in comparison with diesel fuel cost the weighted factor of each objective function should be consequently changed. The effect of variation the relative importance of battery wear cost and diesel fuel cost on the optimal solutions and scheduling are presented in Table (4). As it is shown, when the weighted factor is 0 (higher battery wear cost) the battery is not applied and the demand is supplied by DG. With the increase of weighted factor (higher diesel fuel cost), the battery is applied to supply the demand. Therefore, by increasing the diesel fuel cost the share of battery in supplying the demand can be increased up to 34.18%.

In operation optimization procedure, the operator could select one solution among other optimal solutions regarding the preferences and priorities in operation of HRES. TOPSIS method can be used to rank the optimal solutions using a mathematical model. As it can be seen in Fig. (9), the point P is the positive ideal solution while the point N is the negative ideal solution. The amount of relative closeness (CL_i^+) of Pareto solutions to the ideal solution with their ranking are expressed in Table (5). As the result, point B which has the maximum CL^+ is selected as the best solution while the point A and C obtain the second and third ranks, respectively.

Input profiles such as generation/demand data profiles affect the optimal scheduling. For analyzing the effect of weather data profiles on the optimal schedule of HRES, the sensitivity analysis is performed regarding weather seasonal variations. To this aim, the input weather data profiles are recollected from a sample week in summer (Fig. (10)) and the results are compared with prior results which were related to sample week in winter.

Fig. (11-A) and (11-B) shows the optimal power flows regarding three control variables which are DG power generation and battery charge/discharge power flows for a sample week of winter and summer, respectively. As it is expected, the share of direct renewable energy is dramatically increased by 30% due to higher solar energy potential in summer week. This decreases the diesel fuel consumption and battery net energy consumption. Consequently, the diesel fuel cost and battery wear cost are decreased. Therefore, the total operation cost of HRES will be reduced. However, increasing the length of predicted horizon in summer week (Fig. (11-C)) increases the indirect share of renewable energy (battery discharge) and consequently improve the economic justification of HRES. Table (6) summarizes the results of seasonal sensitivity analysis and increase of the length of predicted horizon on optimization results.

6. Conclusion

A novel energy management system based on multi-objective receding horizon optimization has been proposed in this paper. This methodology uses real time data from an experimental setup which is installed to supply the desired demand of the SUT hybrid renewable energy laboratory. Two objective functions (diesel fuel cost vs. battery wear cost) are considered in multi objective optimization methodology which are implemented into receding horizon optimizer. The energy analysis is performed to evaluate the economic and technical performance of the system. The results of RHO are more effective and feasible in comparison with other conventional optimization procedures. The results show that the prediction horizon which is considered as one of the main parameters in receding horizon optimization procedure can significantly affect the optimal scheduling. Then, the results obtained from a sample week in winter have been compared with a sample week in summer to evaluate the effect of resource variation on operation scheduling of HRES. It is concluded that in a sample week in summer the share of direct renewable energy is superior to a sample week in winter due to higher solar potential in summer. This causes the operation cost of the system to be decreased up to 10%.

References

[1] Merei G, Berger C, Sauer DU. Optimization of an off-grid hybrid PV–Wind–Diesel system with different battery technologies using genetic algorithm. Solar Energy 2013; 97:460-473.

[2] García-Trivino P, Llorens-Iborra F, García-Vazquez CA, Gil-Mena AJ, Fernandez-Ramírez LM, Jurado F. Long-term optimization based on PSO of a grid-connected renewable energy/battery/ hydrogen hybrid system. International Journal of Hydrogen Energy 2014; 39: 10805-10816.

[3] Ashouri A, Fux SS, Benz MJ, Guzzella L. Optimal design and operation of building services using mixed-integer linear programming techniques. Energy 2013; 59:365-376.

[4] Buoro D, Pinamonti P, Reini R. Optimization of a Distributed Cogeneration System with solar district heating. Applied Energy 2014; 124:298-308.

[5] Lee WS, Chen YT, Kao Y. Optimal chiller loading by differential evolution algorithm for reducing energy consumption. Energy and Buildings 2011; 43:599-604.

[6] Ardakani AJ, Ardakani FF, Hosseinian SH. A novel approach for optimal chiller loading using particle swarm optimization. Energy and Buildings 2008; 40:2177-2187.

[7] Chang YC. Optimal chiller loading by evolution strategy for saving energy, Energy and Buildings 2007; 39:437-444.

[8] Papantoniou S, Kolokotsa D, Kalaitzakis K. Building optimization and control algorithms implemented in existing BEMS using a web based energy management and control system. Energy and Buildings 2015; 98:45-55.

[9] Tan Z, Ju LW, Li HH, Li JY, Zhang HJ. A two-stage scheduling optimization model and solution algorithm for wind power and energy storage system considering uncertainty and demand response. Electrical Power and Energy Systems 2014; 63:1057-1069.

[10] Guinot B, Bultel Y, Montignac F, Riu D, Pinton E, Noirot-Le Borgne I. Economic impact of performances degradation on the competitiveness of energy storage technologies e Part 1:

Introduction to the simulation optimization platform ODYSSEY and elements of validation on a PV-hydrogen hybrid system. International Journal of Hydrogen Energy 2013; 38:15219-15232.

[11] Guinot B, Bultel Y, Montignac F, Riu D, Noirot-Le Borgne I. Economic impact of performances degradation on the competitiveness of energy storage technologies e Part 2: Application on an example of PV production guarantee. International Journal of Hydrogen Energy 2013; 38:13702-13716.

[12] Kuznetsova E, Li YF, Ruiz C, Zio E. An integrated framework of agent-based modelling and robust optimization for microgrid energy management. Applied Energy 2014; 129:70-88.

[13] Colson MH, Nehrir CM, Gunderson RW. Multi-agent microgrid power management. In: 18th IFAC world congress 2011:3678-83.

[14] Jun Z, Junfeng L, Jie W, Ngan HW. A multi-agent solution to energy management in hybrid renewable energy generation system. Renewable Energy 2011; 36(5):1352-63.

[15] Cau G, Cocco D, Petrollese M, Kær SK, Milan C. Energy management strategy based on short-term generation scheduling for a renewable microgrid using a hydrogen storage system. Energy Conversion and Management 2014; 87:820-831.

[16] Tsikalakis A, Hatziargyriou N. Centralized control for optimizing microgrids operation. In: IEEE power and energy society general meeting; 2011; 1–8.

[17] Roshandel R, Behzadi Forough A. Two strategies for multi-objective optimisation of solid oxide fuel cell stacks. International Journal of Sustainable Energy 2013; doi: 10.1080/14786451.2013.777337.

[18] Garcia P, Torreglosa JP, Fernandez LM, Jurado F. Optimal energy management system for standalone wind turbine/photovoltaic/hydrogen/battery hybrid system with supervisory control based on fuzzy logic. International Journal of Hydrogen Energy 2013; 38:14146-14158.

[19] García P, Torreglosa JP, Fernández LM, Jurado F. Improving long-term operation of power sources in off-grid hybrid systems based on renewable energy, hydrogen and battery. Journal of Power Sources 2014; 265:149-159.

[20] Tazvinga H, Zhu B, Xia X. Optimal power flow management for distributed energy resources with batteries. Energy Conversion and Management 2015; 102:102-110.

[21] Tazvinga H, Zhu B, Xia X. Energy dispatch strategy for a photovoltaic-wind diesel- battery hybrid power system. Solar Energy 2014; 108:412-20.

[22] Tazvinga H, Xia X, Zhang J. Minimum cost solution of photovoltaic-diesel battery hybrid power systems for remote consumers. Solar Energy 2013; 96:292-9.

[23] Pascual J, Barricarte J, Sanchis P, Marroyo L. Energy management strategy for a renewable-based residential microgrid with generation and demand forecasting. Applied Energy 2015; 158:12-25.

[24] Chen J, Garcia HE. Economic optimization of operations for hybrid energy systems under variable markets. Applied Energy 2016; 177:11-24.

[25] Marzband M, Yousefnejad E, Sumper A, Domínguez-García JL. Real time experimental implementation of optimum energy management system in standalone Microgrid by using multi-layer ant colony optimization. Electrical Power and Energy Systems 2016; 75:265-274.

[26] Ikeda S, Ooka R. A New Optimization Strategy for the Operating Schedule of Energy Systems under Uncertainty of Renewable Energy Sources and Demand Changes. Energy and Buildings 2016; doi: http://dx.doi.org/10.1016/j.enbuild.2016.04.080.

[27] Faeze Brahman F, Honarmand M, Jadid S. Optimal Electrical and Thermal Energy Management of a Residential Energy Hub, Integrating Demand response and Energy Storage System. Energy and Buildings 2014; doi: http://dx.doi.org/10.1016/j.enbuild.2014.12.039.

[28] Alvarado DC, Acha S, Shah N, Markides CN. A Technology Selection and Operation (TSO) optimisation model for distributed energy systems: Mathematical formulation and case study. Applied Energy 2016; 180:491-503.

[29] Chen SM, Cheng SH, Lan TC. Multicriteria decision making based on the TOPSIS method and similarity measures between intuitionistic fuzzy values. Information Sciences 2016; 10.1016/j.ins.2016.05.044.

[30] Shahroudi K, Rouydel R. Using a multi-criteria decision making approach (ANP-TOPSIS) to evaluate suppliers in Iran's auto industry. International Journal of Applied Operational Research 2012; 2(2):37-48.

[31] Li X, Wen J, Ali Malkawi A. An operation optimization and decision framework for a building cluster with distributed energy systems. Applied Energy 2016; 178:98-109.

[32] Di Somma M, Yan B, Bianco N, Luh PB, Graditi G, Mongibello L, Naso V. Multi-objective operation optimization of a Distributed Energy System for a large-scale utility customer. Applied Thermal Engineering 2016; 101:752-761.

[33] Nease J, Adams II TA. Application of rolling horizon optimization to an integrated solid-oxide fuel cell and compressed air energy storage plant for zero-emissions peaking power under uncertainty. Computers and Chemical Engineering 2014; 68:203-219.

[34] Gonzáleza R, Rocab L, Rodrígueza F. Economic optimal control applied to a solar seawater desalination plant. Computers and Chemical Engineering 2014; 71:554-562.

[35] Feroldi D, Rullo P, Zumoffen D. Energy management strategy based on receding horizon for a power hybrid system. Renewable Energy 2015; 75:550-559.

[36] Prodan I, Zio E. A model predictive control framework for reliable microgrid energy Management. Electrical Power and Energy Systems 2014; 61:399-409.

[37] Petrollese M, Valverde L, Cocco D, Cau G, Guerra J. Real-time integration of optimal generation scheduling with MPC for the energy management of a renewable hydrogen-based microgrid. Applied Energy 2016; 166:96-106.

[38] Wang X, Teichgraeber H, Palazoglu A, El-Farra NH. An economic receding horizon optimization approach for energy management in the chlor alkali process with hybrid renewable energy generation. Journal of Process Control 2014; 24:1318-1327.

[39] Wang W, Palazoglu A, El-Farra NH. Operational optimization and demand response of hybrid renewable energy systems. Applied Energy 2015; 143:324-335.

[40] Wang X, El-Farra NH, Palazoglu A. Optimal scheduling of demand responsive industrial production with hybrid renewable energy systems. Renewable Energy 2016; 100:53-64.

[41] Gruber JK, Huerta F, Matatagui P, Prodanovic M. Advanced building energy management based on a two-stage receding horizon optimization. Applied Energy 2015; 160:194-205.

[42] Carapellucci R, Giordano L. Modeling and optimization of an energy generation island based on renewable technologies and hydrogen storage systems. International Journal of Hydrogen Energy 2012; 37:2081-2093.

[43] Sharafi M, ELMekkawy Y. Multi-objective optimal design of hybrid renewable energy systems using PSO-simulation based approach. Renewable Energy 2014; 68:67-79.

[44] Shin Y, Yong Koo W, Hyung Kim T, Jung S, Kim H. Capacity design and operation planning of a hybrid PV-Wind-Battery-Diesel power generation system in the case of Deokjeok Island. Applied Thermal Engineering 2015; 89:514-525.

[45] Binder H, Cronin T, Lundsager P, Manwell JF, Abdulwahid U, Baring-Gould I. Lifetime modelling of lead acid batteries. Technical report. Roskilde, Denmark: Riso National Laboratory; 2005.

[46] Behzadi Forough A, Roshandel R. Multi objective optimization of solid oxide fuel cell stacks considering parameter effects: Fuel utilization and hydrogen cost. J. Renewable Sustainable Energy 2013; 5:053124.

[47] Marler RT, Arora JS. Survey of multi-objective optimization methods for engineering. Struct Multidiscip Optim 2004; 26:369-395.

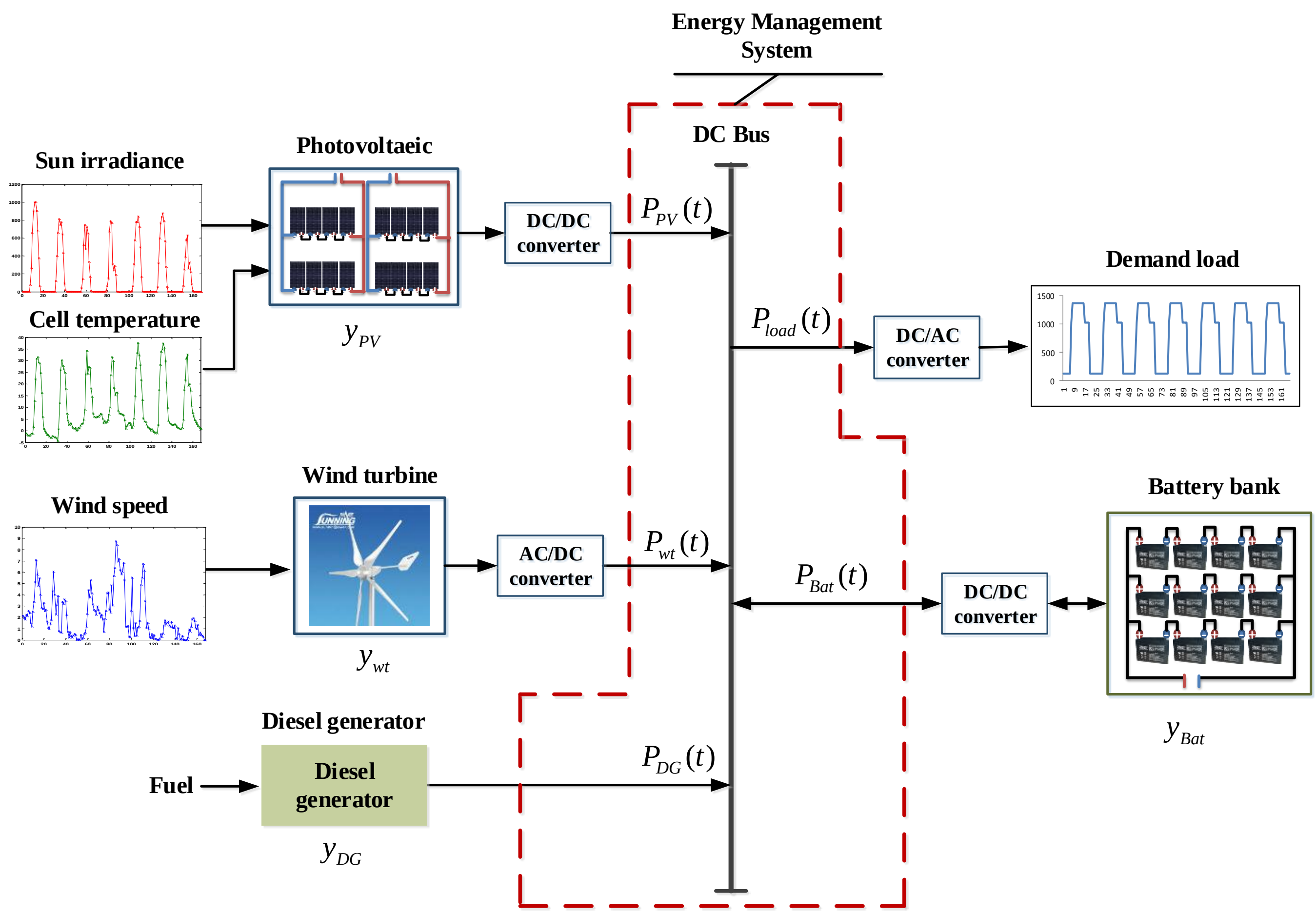

Fig. 1. Schematic diagram of the hybrid renewable energy system (HRES)

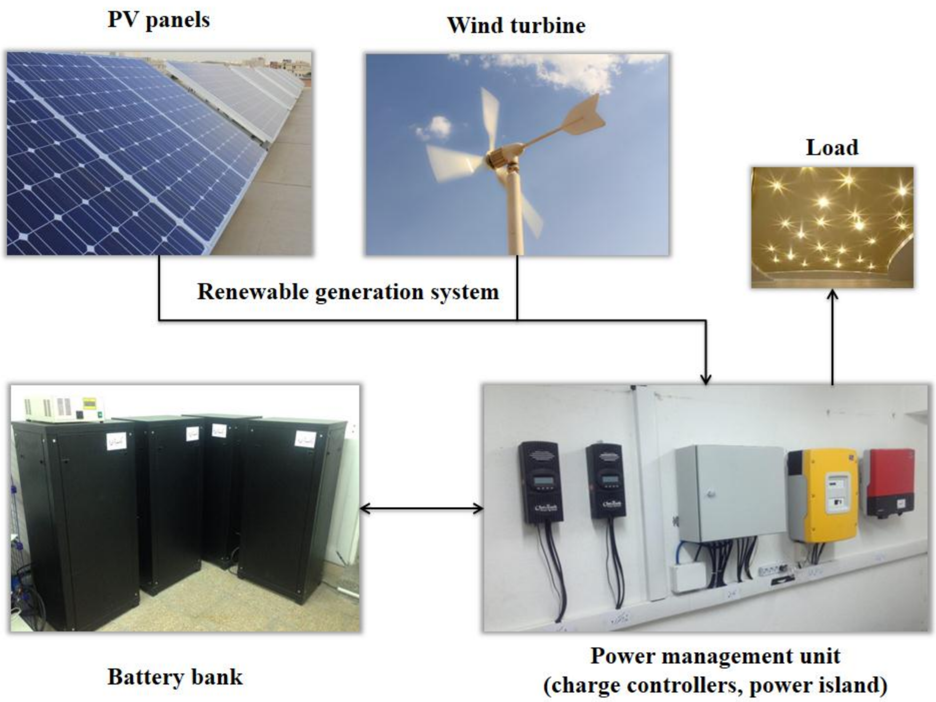

Fig. 2. HRES installed in SUT hybrid renewable energy laboratory

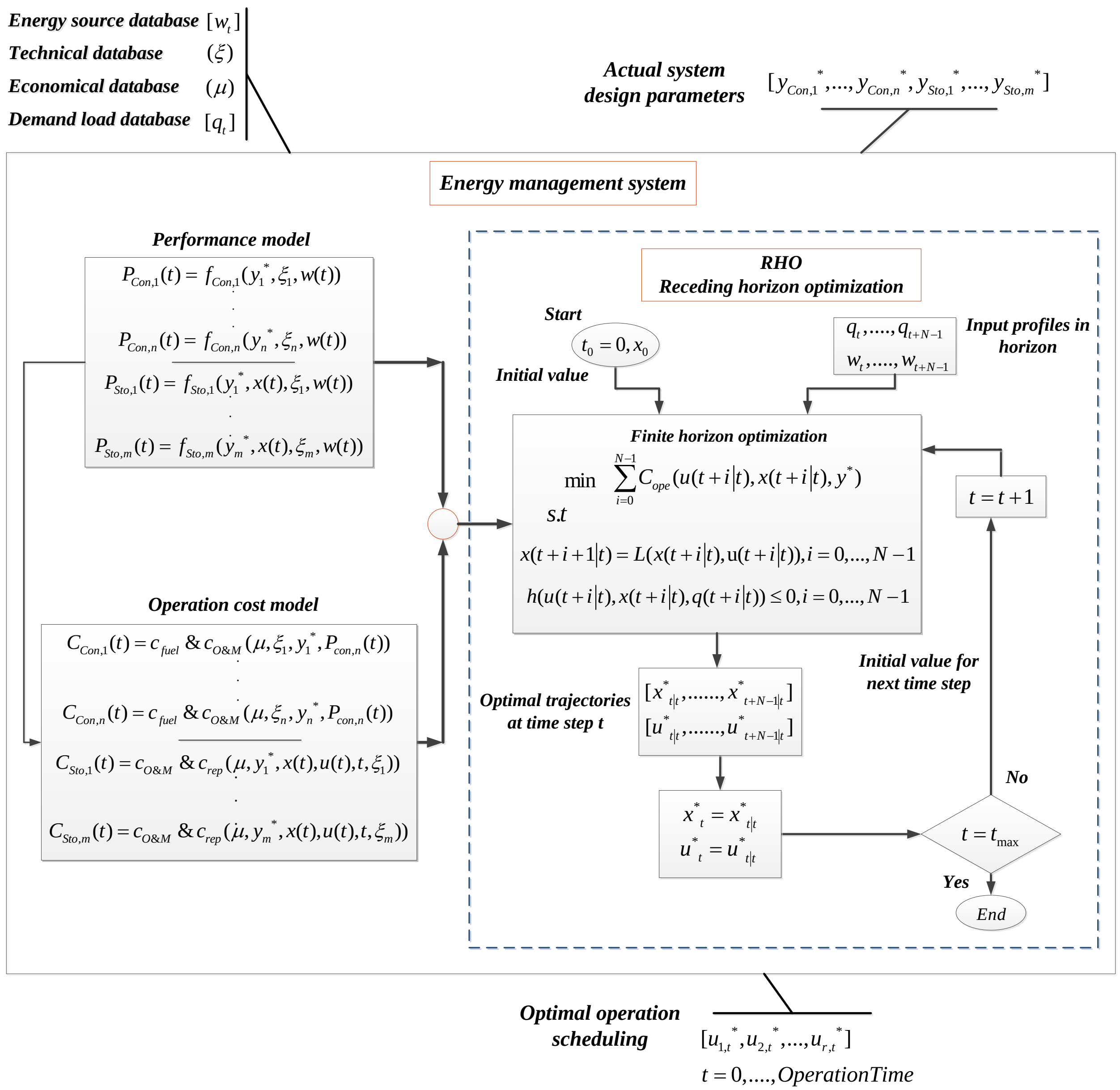

Fig. 3. Mathematical framework of energy management system

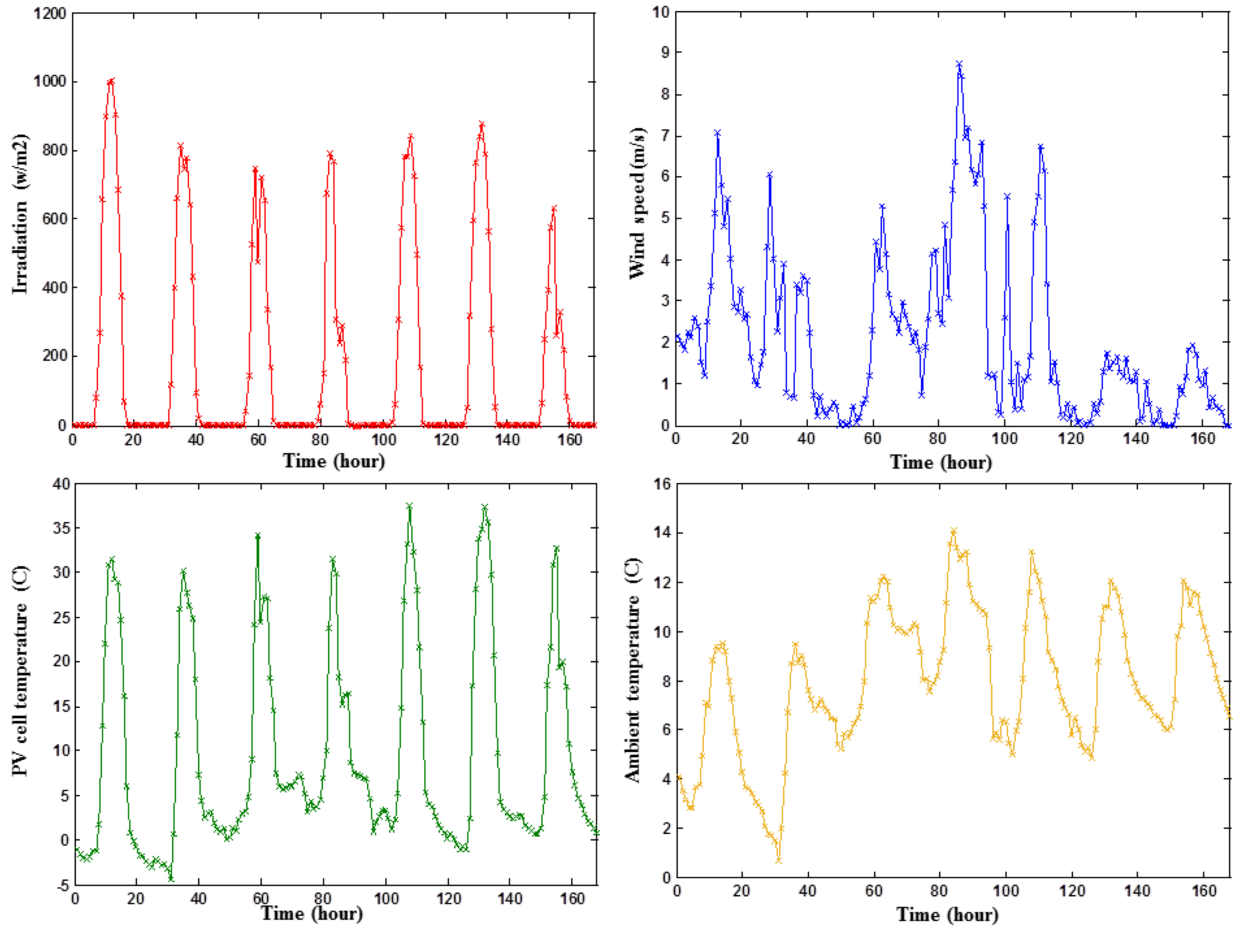

Fig. 4. Measured RHO input weather profiles from sensor box for a winter week

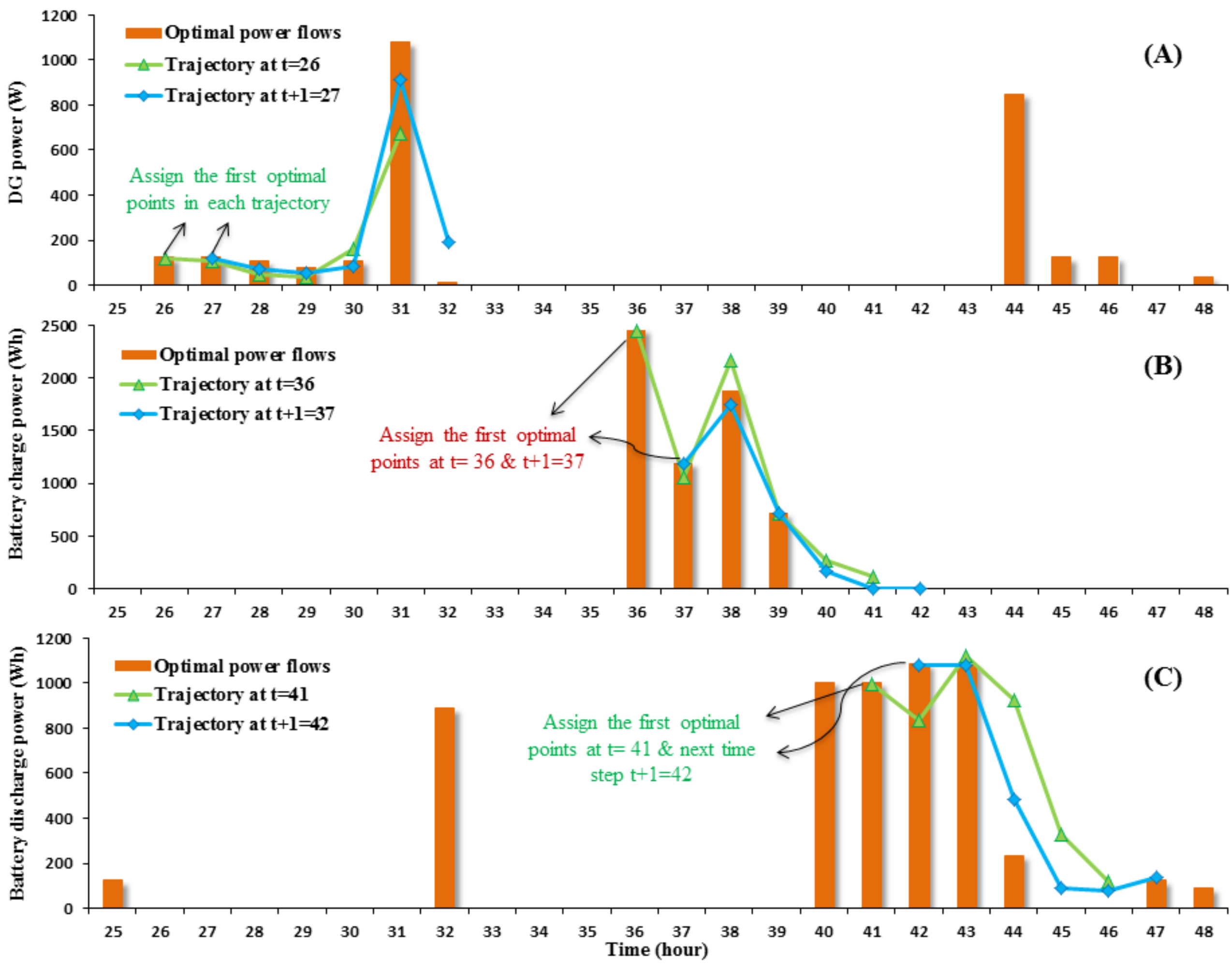

Fig. 5. Illustrative RHO optimal trajectories and implementation using the receding horizon concept. (A), (B) and (C) show the RHO optimal power flows of three control variables

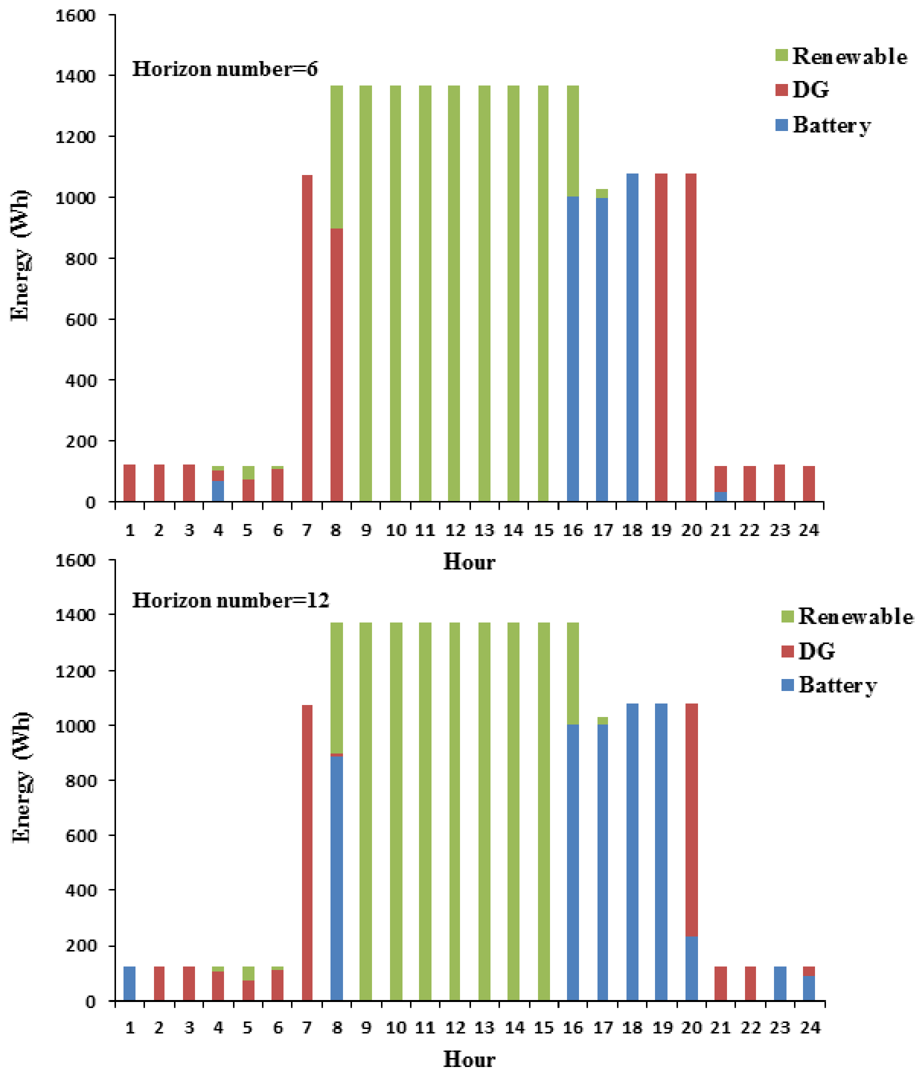

Fig. 6. The optimal share of energy supply side to meet daily demand profile in two length of horizons

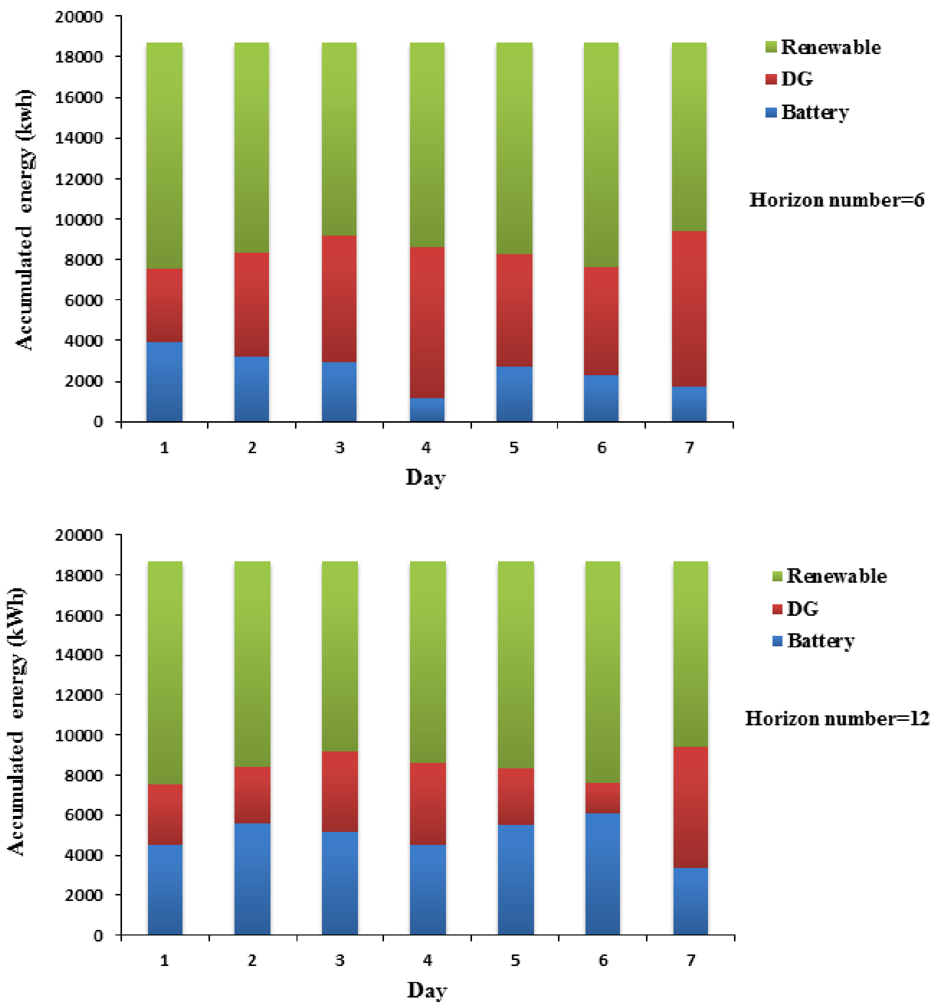

Fig. 7. The accumulated optimal share of energy supply side to meet weekly demand profile in two length of horizons

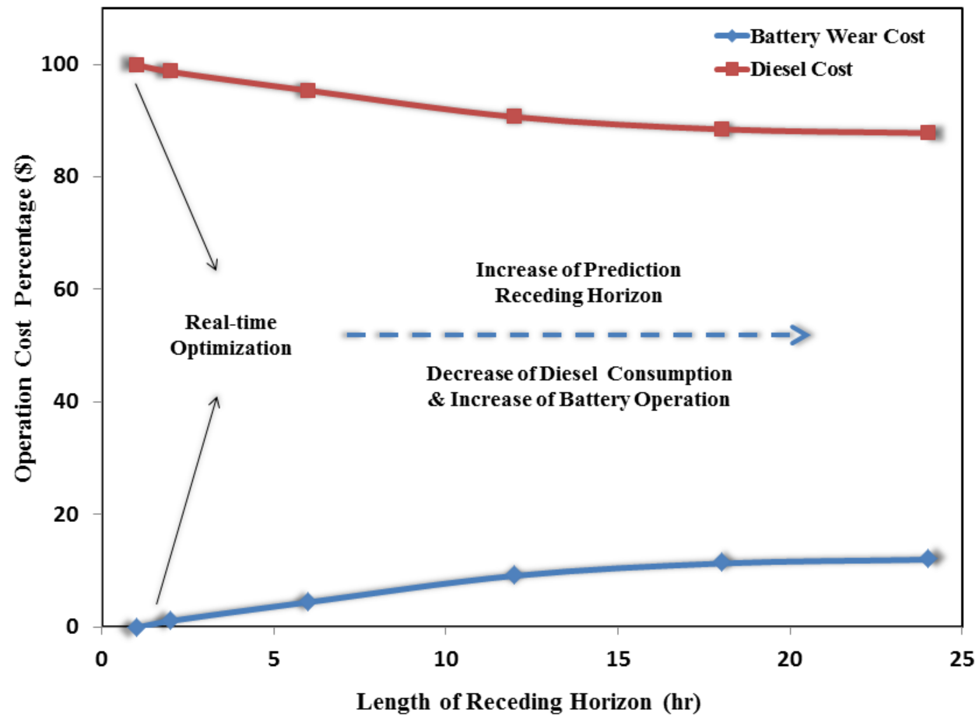

Fig. 8. The effect of receding horizon number on battery wear and fuel cost of HRES

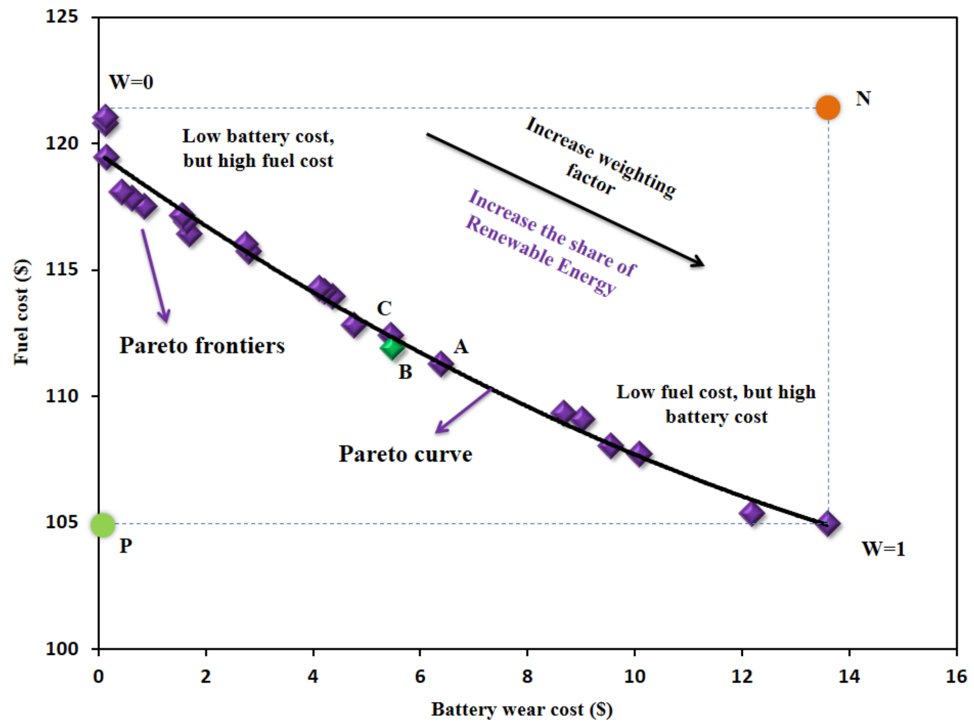

Fig. 9. The Pareto frontiers and Pareto curve: diesel fuel cost vs. battery wear cost

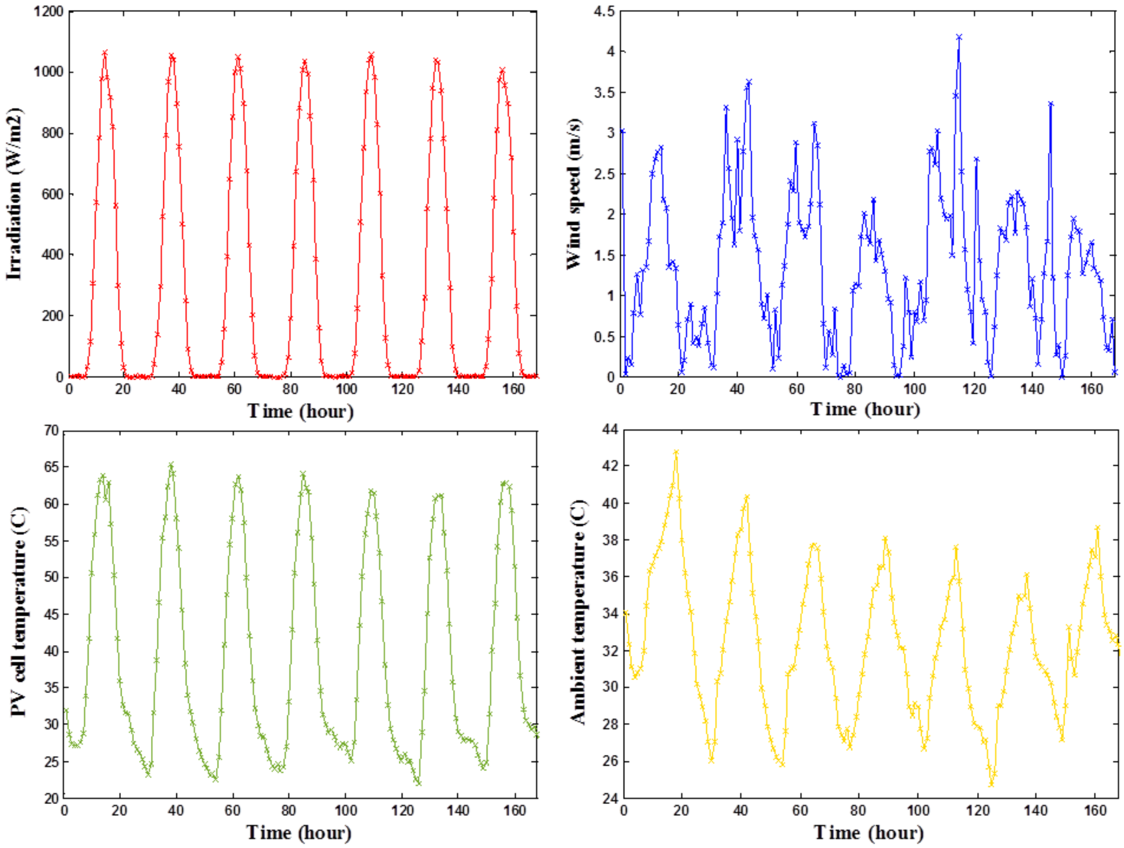

Fig. 10. Measured RHO input weather profiles from sensor box for a summer week

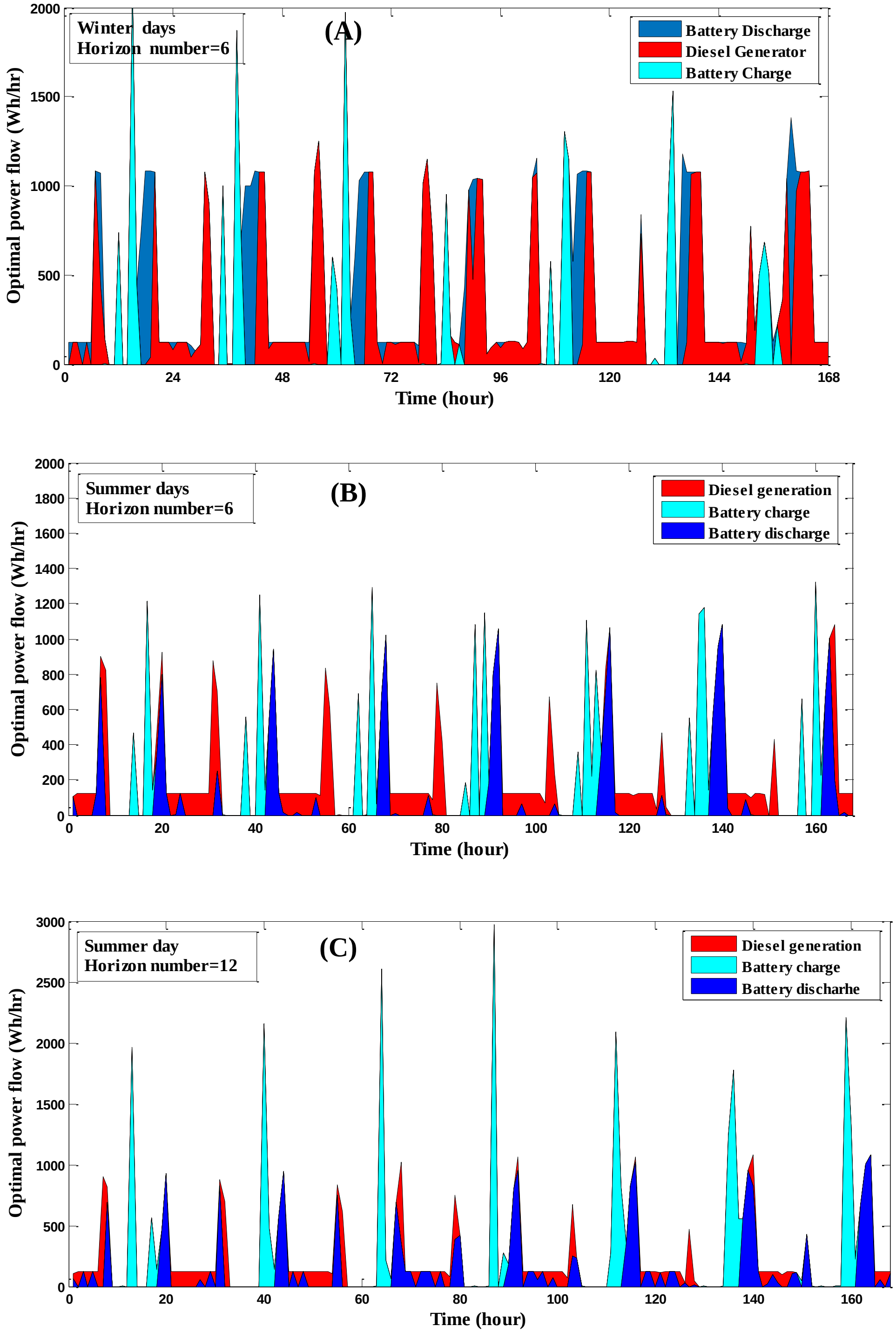

Fig. 11. Optimal power flows (control variables) using RHO concept for a winter/summer week and two length of horizons

Table. 1. The detail of the commercially available HRES devices

Components	Type	Number	Capacity
PV	Sharp NU-E235E2 (235W)	22	5170 W
Wind turbine	Sunning wind turbine (600W)	1	600 W
Charge controllers	Flexmax 60 outback (3000W)	2	-
Battery bank	Narada (100Ah, 12V)	8	9600 Wh
Power island	SMA SI 4850 (48V, 50A)	1	-
Communication interface	Webbox	1	-

Table. 2. Characteristics of installed renewable energy system

Technical parameters		
Parameter	**Value**	**Unit**
Photovoltaic		
$P_{PV,r}$	235	W
η_{PV}	0.14	-
A_{PV}	1.64	m^2
α	0. 485	%/^{0}C
$NOCT$	47	^{0}C
Wind turbine		
$P_{W,r}$	600	W
A_W	2.27	m^2
V_C	2.5	m/s
V_r	12	m/s
V_f	14	m/s

Table. 3. Modeling parameters of battery bank and diesel generator

Technical parameters		
Parameter	**Parameter**	**Parameter**
Diesel generator		
P_{r-DG}	5000	W
α_{DG}	0.081451	Liter/kWh
β_{DG}	0.3058	Liter/kWh
Battery		
τ	0.0002	-
η_{ch}	100	%
η_{dis}	90	%
DOD	20	%
SOC_{max}	100	%
CTF	1400	cycle
Economic parameters [44]		
C_f	1.2	$/Liter
C_{Bat}	750	$/kWh

Table. 4. The variation of optimal solutions with respect to different weighted factors

Weighted factor	**Battery wear cost ($)**	**Diesel fuel cost ($)**	**Total operation cost ($)**	**Share of battery in supplying the demand (%)**
0	0	122.87	122.87	0
0.5	5.45	115.2	120.64	13.67
1	13.59	104.96	118.55	34.18

Table. 5. The relative closeness of Pareto solutions with their ranking in TOPSIS approach

Alternatives	**A**	**B**	**C**
CL_i^+	0.6029	0.6066	0.5900
Ranking	2	1	3

Table. 6. The summarized optimization results for a winter/summer week and two length of horizons

Sample week		**Winter week**		**Summer week**	
Length of horizon		**N=6**	**N=12**	**N=6**	**N=12**
Total load (kWh)		130.76	130.76	130.76	130.76
Direct renewable (kWh)		71.8	71.76	100	100.38
Battery charge (kWh)		18.88	38.74	15.95	22.13
Battery discharge	kWh	17.89	34.66	15.25	20.46
	%	13.68%	26.5%	11.67%	15.64%
Diesel generator (kWh)		41.1	24.34	15.1	9.92
Share of total renewable	kWh	89.6	106.41	116	120.84
	%	68.52%	81.38%	88.7%	92.41%
Share of diesel generator (%)		31.43%	18.61%	11.54%	7.6%
Total operation cost ($)		120.60	118.81	108.48	107.92